Monthly Notices
of the
ROYAL ASTRONOMICAL SOCIETY

Mon. Not. R. Astron. Soc. **418,** 2773–2778 (2011) doi:10.1111/j.1365-2966.2011.19677.x

A magnetar strength surface magnetic field for the slowly spinning down SGR 0418+5729

Tolga Güver,[1⋆] Ersin Göğüş[2] and Feryal Özel[1]

[1]*Department of Astronomy, University of Arizona, 933 N. Cherry Avenue, Tucson, AZ 85721, USA*
[2]*Sabancı University, Faculty of Engineering and Natural Sciences, Orhanlı – Tuzla, İstanbul 34956, Turkey*

Accepted 2011 August 20. Received 2011 August 19; in original form 2011 July 29

ABSTRACT

The observed upper bound on the spin-down rate of the otherwise typical soft gamma-ray repeater SGR 0418+5729 has challenged the interpretation of this source as a neutron star with ultrastrong magnetic fields. Current limits imply a dipole magnetic field strength of less than 7.5×10^{12} G, which is significantly smaller than that of a typical SGR. Independent of the properties inferred from X-ray timing, the X-ray spectra of neutron stars allow a measurement of their magnetic field strengths because they are distorted from pure blackbodies due to the presence of a magnetic field in a radiative equilibrium atmosphere. In this paper, we model high signal-to-noise ratio *XMM–Newton* spectra of SGR 0418+5729 to place constraints on the strength of the magnetic field at the surface of the neutron star. Our analysis shows that neutron star atmosphere models with moderate magnetic field strengths (10^{12-13} G) cannot fit the X-ray spectra, whereas models with stronger magnetic fields are able to account for the observations. We find that the strength of the magnetic field at the surface is 1.0×10^{14} G. This value, although lower than all of the other SGRs analysed to date, is still high enough to generate the observed X-ray bursts from the source. In connection to the spin-down limits, it also implies a significantly non-dipolar structure of the magnetic field. We discuss the results of our spectral modelling and compare them with other SGRs.

Key words: stars: magnetars – stars: neutron – X-rays: individual: SGR 0418+5729.

1 INTRODUCTION

Soft gamma-ray repeaters (SGRs) are neutron stars that are identified by the repeated bursts they emit in hard X-rays and soft gamma-rays. During their burst-active phases, SGRs emit anywhere from a few to thousands of short bursts, typically lasting a fraction of a second. Energy released during such a short time is very large, ranging from $\sim 10^{37}$ to 10^{40} erg. On rare occasions, SGRs emit extremely energetic giant flares, lasting for a few hundreds of seconds and releasing a total energy in excess of 10^{44} erg (Palmer et al. 2005).

SGRs also display persistent bright X-ray emission with luminosities of the order of $L_{\rm X} \lesssim 10^{35}\,{\rm erg\,s^{-1}}$, which significantly exceeds the spin-down power that can be generated by these slowly rotating neutron stars. Both the persistent X-ray emission and the energetic bursts led to the interpretation of SGRs as extremely magnetized neutron stars, or magnetars (Duncan & Thompson 1992; see Woods & Thompson 2006, for a detailed review). Within the magnetar paradigm, the decay of a very strong magnetic field (10^{14}–10^{15} G) powers the persistent emission from SGRs (Thompson & Duncan 1996), while the observed bursts are attributed either to cracking of the neutron crust that is strained by magnetic stress (Thompson & Duncan 1995) or to magnetic reconnection (Lyutikov 2003).

Large period derivatives, of the order of $\dot{P} \simeq 10^{-11}\,{\rm s\,s^{-1}}$, measured from numerous SGRs in the past indicated large inferred dipole spin-down fields $B_{\rm dip} = 10^{14}(P/5\,{\rm s})^{1/2}(\dot{P}/10^{-11}\,{\rm s\,s^{-1}})^{1/2}$ G, thus lending further support to the magnetar character of these sources (e.g. Kouveliotou et al. 1998). When models of high magnetic field neutron star atmospheres (NSAs) and magnetospheres were used to fit to the continuum X-ray spectra of magnetars, these analyses also yielded magnetic field strengths that are comparable to the inferred dipole fields with a typical range of 2–5 $\times$ 10^{14} G (e.g. Güver et al. 2007; Güver, Özel & Göğüş 2008; Özel, Güver & Göğüş 2008; Göğüş et al. 2011; Ng et al. 2011).

The ubiquitous presence of large period derivatives in SGRs is now being challenged by the unusually small period derivative measured in SGR 0418+5729. Early attempts to obtain its period derivative, and therefore to establish its inferred dipolar magnetic field strength, were inconclusive (Kuiper & Hermsen 2009; Woods et al. 2009; Esposito et al. 2010). Using multisatellite observations spanning over 440 d following the onset of the outburst from this

⋆E-mail: tguver@email.arizona.edu

source, Rea et al. (2010) recently reported a 2σ upper limit to the period derivative, implying that the inferred dipolar magnetic field strength of SGR 0418+5729 should be less than 7.5×10^{12} G.

SGR 0418+5729 is a regular SGR in every other way and a transient magnetar candidate (Rea & Esposito 2011): it was discovered on 2009 June 5 by emitting two bursts detected with gamma-ray burst monitor (GBM) on-board *Fermi Gamma-ray Space Telescope* (van der Horst et al. 2010). The energies released by these two events were modest, totalling 8×10^{36} and 4×10^{37} erg in the 20–200 keV band. *Rossi X-Ray Timing Explorer* (*RXTE*) observations of the source following the discovery revealed the 9.07 s spin period (Göğüş, Woods & Kouveliotou 2009). Detectors onboard *Swift*, *Fermi* and *RXTE* have allowed a growing number of transient magnetars to be discovered in the recent years, which are first detected via bursting activity and accompanied persistent flux increase up to several orders of magnitude. Persistent flux of these transient sources decreases back to quiescent level ($\approx 10^{-13}$ erg cm^{-2} s^{-1}) on a time-scale of months to years (Rea & Esposito 2011). X-ray output variation of SGR 0418+5729 also very much resembles that of transient magnetar candidates: the 1–10 keV flux rapidly increased in conjunction with bursting and subsequently decayed by a factor of 10 over a time-span of $\sim$150 d (Esposito et al. 2010). SGR 0418+5729 is located towards the Galactic anticentre and likely to be in the Perseus arm or the outer arm of our Galaxy with a distance of $\approx$2 kpc or higher (van der Horst et al. 2010).

In this paper, we aim to place constraints on the magnetic field strength of SGR 0418+5729 using X-ray spectroscopy. To this end, we analyse the high signal-to-noise ratio X-ray spectrum of SGR 0418+5729 obtained from *XMM–Newton* observations. We use a number of different X-ray spectral models to constrain the physical properties of the neutron star. In particular, we employ (i) the phenomenological blackbody plus power-law (PL) model that has been traditionally used to fit SGR spectra, (ii) the low-to-moderate magnetic field NSA model (Pavlov et al. 1995; Zavlin, Pavlov & Shibanov 1996) and (iii) the high magnetic field surface thermal emission and magnetospheric scattering (STEMS) model (Güver et al. 2007, 2008). We find that the thermal spectrum of SGR 0418+5729 is best described by high magnetic field model. We also compare the magnetic field determined spectroscopically to the dipole magnetic field inferred from spin-down. Because the spectroscopically determined field probes the strength measured on the neutron star surface, whereas the dipole field is the one inferred at the light cylinder, this comparison can be revealing for the field geometry of SGR 0418+5729.

We introduce the *XMM–Newton* data and our data reduction procedure in the next section. In Section 3, we fit the spectrum with the three different continuum models. Finally, we discuss the implications of the inferred surface magnetic field strength and compare our findings for this source with those of SGRs in general to address the possible differences between them in the final section.

2 OBSERVATIONS AND DATA ANALYSIS

In the period following its discovery through its X-ray/soft gamma-ray bursts, SGR 0418+5729 could not be observed immediately with pointing telescopes due to its unfavourable sky location. In particular, *Swift* X-ray Telescope observations of the source could start about a month after the discovery, while the *XMM–Newton* observation was performed about two months after. Because the X-ray intensity of the source steadily declined following the outburst (see fig. 1 of Esposito et al. 2010), only the large collecting area of *XMM–Newton* was able to provide sufficiently high-quality X-ray spectrum for the measurement of spectral parameters. We, therefore, use in this study the archival *XMM–Newton* observation that took place on 2009 August 12 (Obs ID. 0610000601). We note that SGR 0418+5729 was still not in quiescence during the *XMM–Newton* observation (Esposito et al. 2010). During this observation, the source count rate as observed with the European Photon Imaging Camera (EPIC-pn) and MOS detectors were 1.35 and 0.5 count s^{-1}, respectively. EPIC-pn and MOS detectors were operated in small and partial window modes with time resolutions of 6 and 300 ms, respectively, to prevent photon pile-up.

Part of the *XMM–Newton* observation, especially towards the end, was severely affected by large particle flares. We are, therefore, able to use $\approx$36 ks out of the total exposure time of 65 ks. We utilize data collected with both the EPIC-pn and EPIC-MOS cameras.

We used the *epproc* and *emproc* tasks for the EPIC-pn and EPIC-MOS data with the Science Analysis Software (SAS) version 10.0.0 and the latest available calibration files as of 2010 December. We extracted X-ray spectra using a circular region with a radius of 32 arcsec centred on the source. Similarly, background regions were selected from a source-free region with a typical radius of 50 arcsec. We used the *rmfgen* and *arfgen* tools to create response and ancillary response files. We rebinned the X-ray spectra to have at least 30 count bin^{-1} and not to oversample the intrinsic energy resolution of the detectors by more than a factor of 3.

3 X-RAY SPECTRAL ANALYSIS AND RESULTS

We fit the data with XSPEC version 12.5.1n (Arnaud 1996). In all the fits, we used the *tbabs* model and the interstellar medium abundances (Wilms, Allen & McCray 2000) to account for the effects of interstellar absorption. The *XMM–Newton* calibration team reported that the EPIC-MOS detectors measure 5–8 per cent higher fluxes than the EPIC-pn consistently over the whole energy band.[1] However, the exact amount of this excess flux varies over different energy ranges. Therefore, in all our fits we allowed the normalization parameters of the models to be free between the detectors and added a 1 per cent systematic uncertainty to take into account the possible energy dependence of the uncertainties in instrumental calibrations. We calculated the unabsorbed flux using the *cflux* model in XSPEC. Because of the above-mentioned calibration uncertainty, we only report the flux and/or emitting area values as measured with EPIC-pn. We assumed a gravitational redshift for the neutron star as 0.25, corresponding to a neutron star mass of 1.4 $M_\odot$ and radius of 11.5 km. We fit all spectra in the 0.5–6.5 keV energy range. Unless otherwise noted, all the uncertainties quoted are for 68 per cent confidence interval.

We first fit the X-ray spectra using a combination of a blackbody (*bbodyrad* as defined in XSPEC) and a PL model. We performed this analysis only as a phenomenological classification of the source spectrum because the atmospheric structure even for a weak or 'zero' magnetic field has a strong effect on the spectral shape of the X-ray emission of neutron stars and has been shown to distort it away from a blackbody (see e.g. Romani 1987; Pavlov et al. 1995). The spectrum and the best-fitting model are shown in the left-hand panel of Fig. 1. Blackbody plus PL provided a moderate fit with a χ^2/degrees of freedom (d.o.f.) of 1.12 for 346 d.o.f. The best-fitting model resulted in a hydrogen column density of $(1.10 \pm 0.05) \times 10^{22}$ cm^2, a blackbody temperature of 0.93 ± 0.006 keV and a photon index of the PL component of 3.18 ± 0.19. The temperature

[1] See e.g. http://xmm.vilspa.esa.es/docs/documents/CAL-TN-0018.pdf

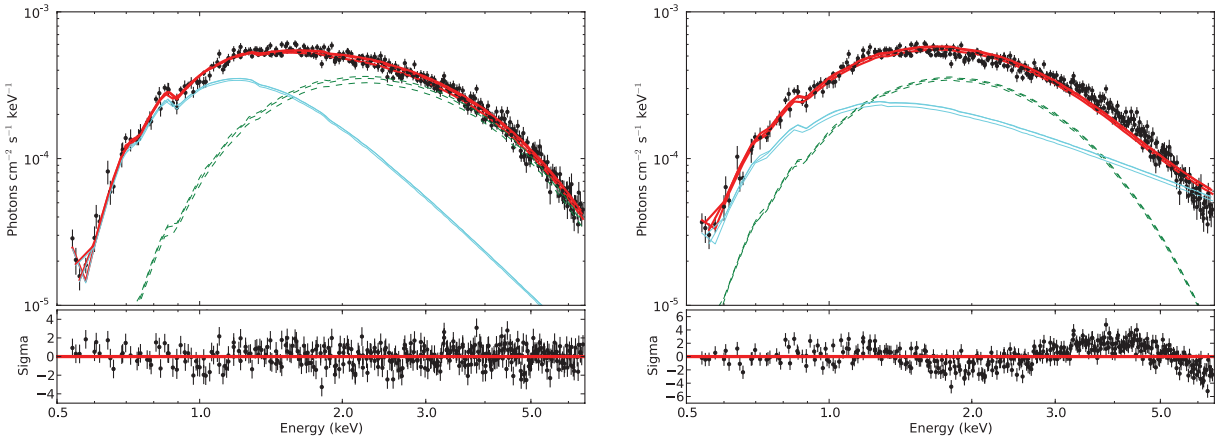

Figure 1. Best-fitting fluxed blackbody + PL (upper left-hand panel) and NSA + PL (upper right-hand panel) fit to the X-ray spectrum of SGR 0418+5729 obtained with the *XMM–Newton*. The magnetic field strength in the NSA model is set to 10^{12} G. Blackbody + PL provides a moderate fit with χ^2/d.o.f. = 1.12 for 346 d.o.f., while the NSA + PL is a poor fit with χ^2/d.o.f. = 2.78 for 346 d.o.f. In both cases, the thermal component dominates (shown with dashed green lines) over the PL component (shown with thick cyan lines) at high photon energies, i.e. in the >1.5 keV range, which is difficult to interpret physically. Lower panels show the residuals from each fit, respectively.

is unusually high for two reasons. First, the blackbody component dominates over the PL component at high photon energies, i.e. in the >1.5 keV range, as can be seen in Fig. 1, which is physically difficult to interpret and is also contrary to what is seen in the spectra of other SGRs. Secondly, this high temperature corresponds to an extremely small emitting radius of 0.18 km per 2 kpc. Such a small emitting radius is especially hard to interpret given the observed pulsed fraction of 20–40 per cent in the soft X-rays (Esposito et al. 2010).

The current constraints on the period derivative of SGR 0418+5729 point to a dipolar magnetic field strength smaller than 7.5×10^{12} G. We, therefore, tried to fit the spectrum of SGR 0418+5729 with low-to-intermediate magnetic field strength NSA models. The NSA model (Pavlov et al. 1995; Zavlin et al. 1996) provides a model for the X-ray spectra emitted from a hydrogen atmosphere of a neutron star at three different magnetic field strengths: $B < 10^8$–10^9 G, $B = 10^{12}$ and 10^{13} G. The fit parameters of the NSA model, in addition to the magnetic field strength, are the neutron star mass and radius, the surface temperature and the normalization, which is a function of the source distance $1/D^2_{\rm kpc}$.

We consider the $B < 10^8$ G case only for completeness, because it would be unfeasible to account for the X-ray pulsations observed from SGR 0418+5729 if indeed possessed a negligible magnetic field. For this case, the NSA model does not provide a good fit with a χ^2/d.o.f. equal to 1.29 for 350 d.o.f. and yields a best-fitting surface temperature of 0.73 keV (8.5×10^6 K). As with the blackbody plus PL fit, this rather high temperature corresponds to a very small best-fitting normalization of 3.0×10^{-10}, or equivalently an emitting radius of $R = 0.4$ km per 2 kpc.

At a field strength of $B = 10^{12}$ G, the NSA model cannot fit the spectrum of SGR 0418+5729, yielding a minimum χ^2/d.o.f. = 13.88 for 350 d.o.f. The surface temperature also hits 10^7 K, which is the maximum of the allowed range in the models. Finally, the obtained best-fitting normalization of 8.5×10^{-11} translates to an unphysically small emitting radius of $R = 0.21$ km per 2 kpc. This indicates that the spectrum of SGR 0418+5729 is inconsistent with a surface magnetic field strength that is comparable to its dipole field strength inferred from its period derivative.

We performed a final NSA fit, where we set the magnetic field strength to $B = 10^{13}$ G. The quality of the fit improved compared to the 10^{12} G case but is still not adequate, yielding a χ^2/d.o.f. = 3.88 for 350 d.o.f. The best-fitting temperature again hits the upper limit of the allowed range at 10^7 K (0.86 keV), corresponding to a normalization of 1.3×10^{-10}, which is an emitting radius of $R = 0.3$ km per 2 kpc.

In an attempt to obtain statistically better fits and to investigate whether additional spectral components would have an effect on the measured effective temperature values, we also modelled the X-ray spectrum of SGR 0418+5729 with an absorbed NSA plus a PL model. We found that the addition of the PL component statistically improved the fits, yielding χ^2/d.o.f. values of 1.13, 2.78 and 1.49 for 346 d.o.f., when the magnetic field strength was set to 0, 10^{12} and 10^{13} G, respectively. However, the addition of the PL component did not decrease the inferred effective temperature, resulting in values that still reached the upper temperature limit of the model. In the right-hand panel of Fig. 1, we show the X-ray spectra and an example case for the NSA+PL models, where the strength of the magnetic field was set to 10^{12} G.

We finally modelled the spectrum of SGR 0418+5729 with magnetar strength fields in the few $\times 10^{13}$–10^{15} G range, which may reflect the higher multipole field strengths present at the stellar surface. To this end, we used the STEMS model (see Güver et al. 2007, 2008). STEMS takes into account the effects of the ultrastrong magnetic fields on the fully ionized hydrogen atmospheres of magnetars (Özel 2001, 2003) and the resonant cyclotron scattering of the surface photons by mildly relativistic charges in the magnetosphere (Lyutikov & Gavriil 2006). For the calculation of the surface emission, we follow Özel (2001, 2003) and solve the radiative transfer equations in a polarization-mode-dependent manner including the absorption, emission and scattering processes in the atmosphere. We also take into account the effects of vacuum polarization resonance and include the interaction of photons with protons in the plasma, which gives rise to absorption features at the proton cyclotron energy (Özel 2003). In the stellar magnetosphere, we incorporate a treatment of resonant cyclotron scattering, following Lyutikov & Gavriil (2006). Resonant cyclotron scattering can take place in a neutron star magnetosphere as long as there is a sufficient density of moderately relativistic electrons and the resulting up-scattering shifts the initial spectrum to higher energies and smears out the proton cyclotron features (Lyutikov & Gavriil 2006).

In the STEMS model, we use the emission emerging from the surface as input for the resonant cyclotron scattering model to obtain the resulting energy distribution of photons. In total, STEMS depends on four parameters: the surface effective temperature ($kT = 0.1$–0.6 keV), the strength of the magnetic field at the surface ($B = 0.6$–50×10^{14} G), the optical depth to scattering in the magnetosphere ($\tau = 1.0$–12.0) and the velocity of the particles in the magnetosphere ($\beta = 0.1$–0.7). Note that, even though in the calculations of Lyutikov & Gavriil (2006) a high optical depth is motivated by a twist angle, this is not a necessary assumption. Such high charge densities are seen in the magnetospheres of even normal pulsars and the only difference between the SGR 0418+5729 and a neutron star with a magnetar-strength dipole field would be the occurrence of the resonant layers closer to the neutron star surface. As an example, based on the current limit on the dipole field of SGR 0418+5729, the resonant layer would be at $4\,R_{\rm NS}$, whereas for a quadrupole field that is 10^{14} G at the surface the resonant layer would be at $\approx 6\,R_{\rm NS}$. Finally, we take into account general relativistic effects on the propagation of the photons by assuming a gravitational redshift.

Compared to the blackbody plus a PL fit, STEMS model provided an equally good fit to the *XMM–Newton* spectrum, resulting in a χ^2/d.o.f. of 1.18 for 347 d.o.f. We show the best-fitting model curve and the X-ray spectra in Fig. 2 . The parameters of the best-fitting model were: the surface magnetic field strength $B = (1.00^{+0.02}_{-0.01}) \times 10^{14}$ G, the surface effective temperature $kT = 0.246^{+0.003}_{-0.01}$ keV, the scattering optical depth in the magnetosphere $\tau = 8.94^{+1.18}_{-0.18}$ and the particle velocity in the magnetosphere $\beta = 0.56 \pm 0.01$. The inferred optical depth and the average electron velocity are well within the assumptions of the resonant cyclotron scattering model (see e.g. section 3.4 of Lyutikov & Gavriil 2006). We also found a hydrogen column density of $(0.74 \pm 0.02) \times 10^{22}$ cm^2 and the unabsorbed 0.5–6.5 keV source flux as $(8.53^{+0.05}_{-0.06}) \times 10^{-12}$ erg s^{-1} cm^{-2}. The inferred emitting radius corresponding to this effective temperature and flux is $R = 2.98$ km per 2 kpc. We note that in this fit fractional emitting area, i.e. $A_{\rm hot}/A_{\rm NS}$, where $A_{\rm NS}$ is the entire neutron star surface area, is in the right range to produce the pulsed fraction of 20–40 per cent, as observed by Esposito et al. (2010) in the soft X-rays.

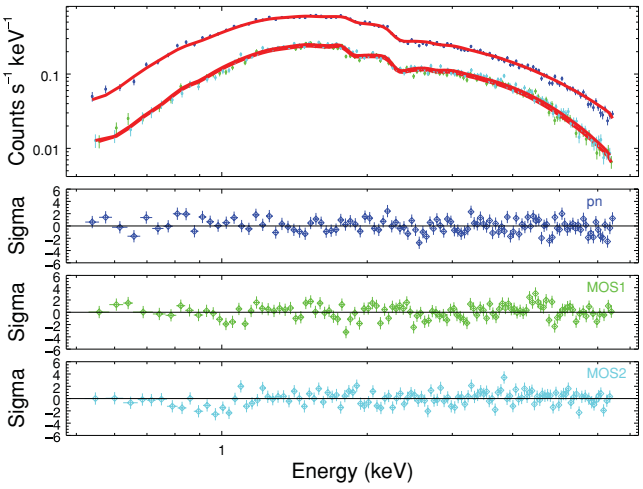

Figure 2. *XMM–Newton* EPIC-pn (blue) and EPIC-MOS (green and cyan) spectra of the SGR 0418+5729. Best-fitting STEMS model is also shown with red thick lines. Residuals from the model for each detector are shown in lower panels.

We present in Fig. 3 the confidence contours of the best-fitting effective temperature and the magnetic field strength at the surface of the neutron star. From the confidence contours, it can clearly be seen that the STEMS model provides a lower limit to the surface magnetic field strength of the neutron star of $\approx 1 \times 10^{14}$ G. Because our focus in this paper is the surface magnetic field strength of SGR 0418+5729, we further explored the uncertainty in this parameter by doing the following. We fit the data by freezing the magnetic field at 1000 different points within the 0.6–4.0×10^{14} G range and allowing the other parameters to vary. Fig. 3 shows the variation of the χ^2/d.o.f. over the full magnetic field range investigated. It is evident from the distinct minimum in the χ^2 in this figure that the magnetic field strength at the surface of the neutron star is uniquely constrained and is found to be 1.0×10^{14} G.

4 DISCUSSION

The recent discovery and the subsequent observations of SGR 0418+5729 have raised a number of questions on our understanding of the SGRs and anomalous X-ray pulsars (AXPs), especially owing to a lack of secular evolution in its spin period. A number of explanations, both within and outside the context of the magnetar model, have been proposed to interpret the peculiarity of SGR 0418+5729. For example, the effects of a stronger toroidal magnetic field below the surface on the neutron star crust were employed to create the observed X-ray bursts independent of strength of the dipole component (see e.g. Rea et al. 2010; Perna & Pons 2011). The existence of a fallback disc has been proposed to evolve the neutron star to its current spin period with a dipole field as low as 10^{12-13} G (Alpar, Ertan & Çalışkan 2011; see also Ertan et al. 2007).

In this paper, we analysed the X-ray spectrum of SGR 0418+5729 to constrain its surface magnetic field strength, as well as the temperature and the magnetospheric parameters of the neutron star. We find that the empirical blackbody + PL model provides a moderate fit, but the emitting area inferred from this fit is unphysically small ($R = 0.18$ km per 2 kpc). In addition, contrary to the physical expectations and in contrast to other AXP and SGR spectra, the blackbody component dominates over the PL component in the higher, as opposed to the lower, energy regime. We also found that realistic atmosphere models of a neutron star with moderate magnetic field strengths (NSA) do not describe the spectrum adequately, yielding χ^2/d.o.f. ≥ 3.9. In contrast, NSA model with magnetar-strength fields (STEMS) produces a fit with χ^2/d.o.f. $= 1.18$ for 347 d.o.f. The best-fitting value of the magnetic field strength is 1.0×10^{14} G. Thus, the spectral analysis strongly disfavours X-ray models where the magnetic field strength at the surface is assumed to be 10^{8-9}, 10^{12} or 10^{13} G.

X-ray observations of a number of other magnetars have been successfully modelled with NSAs with high magnetic field strengths, including XTE J1810−197 (Güver et al. 2007), 4U 0142+61 (Güver et al. 2008), 1E 1048.1−5937, 1RXS J170849.0−400910 (Özel et al. 2008), 1E 1547.0−5408 (Ng et al. 2011) and SGR 1900+14 (Göğüş et al. 2011), and were used to obtain the surface parameters of the neutron stars such as their magnetic field strengths and effective temperatures. The spectroscopically inferred magnetic field strength values for these sources, in units of 10^{14} G, are 2.77 ± 0.05, 4.75 ± 0.03, 2.26 ± 0.05, 3.96 ± 0.17, 3.1 ± 0.5 and 5.0 ± 0.48, respectively. In Fig. 4 , we compare these spectroscopically determined field strengths with the previously reported inferred dipole magnetic field for each source, which we obtained

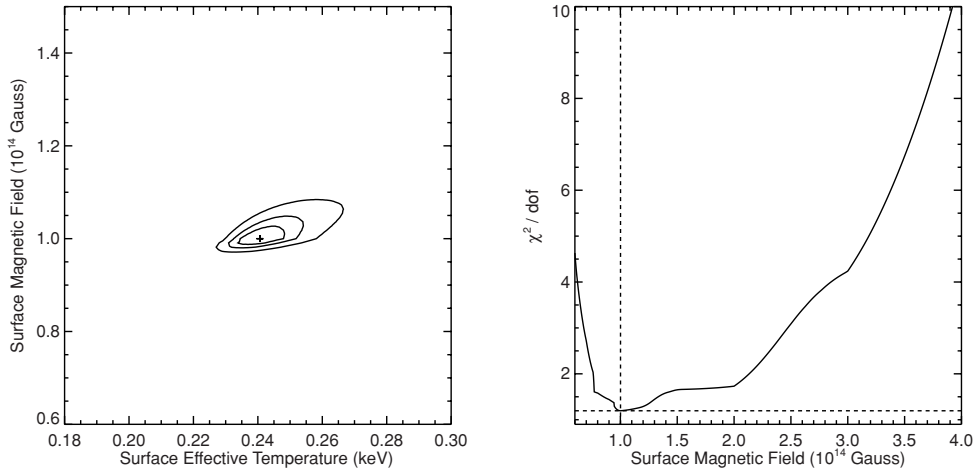

Figure 3. Left-hand panel: confidence contours of the best-fitting surface effective temperature and the magnetic field strength at the surface of the neutron star as inferred from the STEMS model. Right-hand panel: variation of the χ^2/d.o.f. with the surface magnetic field strength. Horizontal and vertical dashed lines show χ^2/d.o.f. and surface magnetic field strength for the best-fitting model.

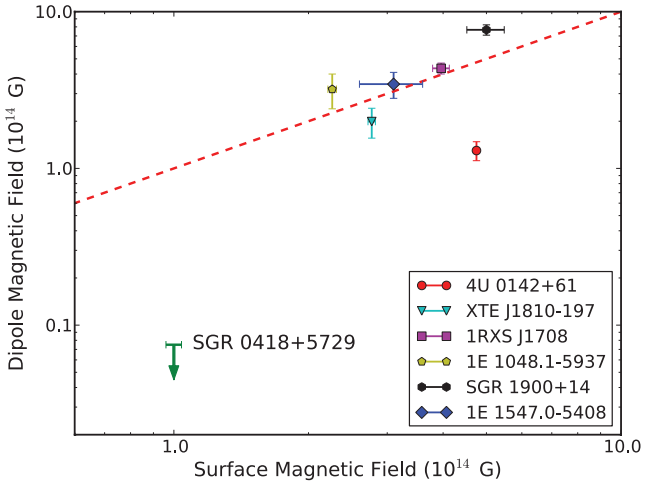

Figure 4. Comparison of the magnetic field strengths as inferred using the STEMS model to the dipole fields deduced from the spin-down properties for seven magnetar candidates. The error bars in dipole field strengths represent the range of measured spin-down rates for each source, while the error bars in the spectroscopic magnetic field strength represent 2σ statistical uncertainties. Dashed lines show the relation where $B_{\rm surf} = B_{\rm dip}$.

from the McGill SGR/AXP Catalog,[2] Ng et al. (2011) and Özel et al. (2008). For all of these sources, the spectrally inferred surface magnetic field strength is in good agreement with dipole magnetic field estimates, differing at most by a factor of 4. SGR 0418+5729 is the first magnetar candidate for which the surface magnetic field strength is significantly larger than the limit on the dipole magnetic field ($\geq$15 times larger). It is also interesting that the surface magnetic field strength we report here for SGR 0418+5729 is the lowest among other STEMS measurements for other AXPs and SGRs so far.

Even though the dipole field strengths inferred from spin-down involve a number of simplifying assumptions, relaxing them in realistic simulations leads to a factor of 2 difference in the inferred magnetic field strengths (Contopoulos & Spitkovsky 2006). Therefore, the discrepancy between the field strength inferred from the spin-down of SGR 0418+5729 and the field strength inferred from both its spectrum and its bursts is too large to be accounted for in this way. Instead, the difference points to a complex magnetic field geometry, i.e. it can be attributed to the presence of higher order multipole components at the surface of the neutron star, which can shape the characteristics of the X-ray emission but do not contribute to the spin-down. The multipole fields are likely to play a role in determining the pulse shapes observed in AXPs and SGRs (Özel 2002). In this interpretation, the higher order components of the magnetic field can also cause the fracturing of the neutron star crust, leading to the observed X-ray bursts. Further comparisons of the surface and dipole magnetic field strengths of AXPs and SGRs, as well as numerical simulations of the magnetic field evolution in young neutron stars, may help further constrain the magnetic field strengths and geometries of X-ray bright neutron stars.

[2] http://www.physics.mcgill.ca/pulsar/magnetar/main.html

ACKNOWLEDGMENTS

We thank the anonymous referee for his/her comments that improved the clarity of the manuscript. This work makes use of observations obtained with *XMM–Newton*, an ESA science mission with instruments and contributions directly funded by ESA Member States and NASA. FÖ and TG acknowledge support from NSF grant AST-07-08640.

REFERENCES

Alpar M. A., Ertan Ü., Çalışkan Ş., 2011, ApJ, 732, L4
Arnaud K. A., 1996, in Jacoby G. H., Barnes J., eds, ASP Conf. Ser. Vol. 101, Astronomical Data Analysis Software and Systems V. Astron. Soc. Pac., San Francisco, p. 17
Contopoulos I., Spitkovsky A., 2006, ApJ, 643, 1139
Duncan R. C., Thompson C., 1992, ApJ, 392, L9
Ertan Ü., Erkut M. H., Ekşi K. Y., Alpar M. A., 2007, ApJ, 657, 441
Esposito P. et al., 2010, MNRAS, 405, 1787
Göğüş E., Woods P., Kouveliotou C., 2009, Astron. Telegram, 2076, 1
Göğüş E., Güver T., Özel F., Eichler D., Kouveliotou C., 2011, ApJ, 728, 160
Güver T., Özel F., Göğüş E., Kouveliotou C., 2007, ApJ, 667, L73
Güver T., Özel F., Göğüş E., 2008, ApJ, 675, 1499
Kouveliotou C. et al., 1998, Nat, 393, 235

Kuiper L., Hermsen W., 2009, Astron. Telegram, 2151, 1
Lyutikov M., 2003, MNRAS, 346, 540
Lyutikov M., Gavriil F. P., 2006, MNRAS, 368, 690
Ng C.-Y. et al., 2011, ApJ, 729, 131
Özel F., 2001, ApJ, 563, 276
Özel F., 2002, ApJ, 575, 397
Özel F., 2003, ApJ, 583, 402
Özel F., Güver T., Göğüş E., 2008, in Bassa C., Wang Z., Cumming A., eds, AIP Conf. Proc. Vol. 983, 40 Years of Pulsars: Millisecond Pulsars, Magnetars and More. Am. Inst. Phys., New York, p. 254
Palmer D. M. et al., 2005, Nat, 434, 1107
Pavlov G. G., Shibanov Y. A., Zavlin V. E., Meyer R. D., 1995, in Alpar M. A., Kiziloglu U., van Paradijs J., eds, Proc. NATO Advanced Study Inst., The Lives of the Neutron Stars. Kluwer, Dordrecht, p. 71
Perna R., Pons J. A., 2011, ApJ, 727, L51
Rea N., Esposito P., 2011, in Torres D. F., Rea No., eds, Astrophys. Space Sci. Proc., High-Energy Emission from Pulsars and their Systems. Springer, Berlin, p. 247
Rea N. et al., 2010, Sci, 330, 944
Romani R. W., 1987, ApJ, 313, 718
Thompson C., Duncan R. C., 1995, MNRAS, 275, 255
Thompson C., Duncan R. C., 1996, ApJ, 473, 322
van der Horst A. J. et al., 2010, ApJ, 711, L1
Wilms J., Allen A., McCray R., 2000, ApJ, 542, 914
Woods P. M., Thompson C., 2006, in Lewin W., van der Klis M., eds, Compact Stellar X-ray Sources. Cambridge Univ. Press, Cambridge, p. 547
Woods P. M. et al., 2009, Astron. Telegram, 2152, 1
Zavlin V. E., Pavlov G. G., Shibanov Y. A., 1996, A&A, 315, 141

This paper has been typeset from a TEX/LATEX file prepared by the author.